International Journal of Refractory Metals and Hard Materials 116 (2023) 106346

Contents lists available at ScienceDirect

International Journal of Refractory Metals and Hard Materials

journal homepage: www.elsevier.com/locate/IJRMHM

On the constitution and cobalt alloy formation in WC-1.4 wt% Ru-9.5 wt% Co cemented carbides

W.D. Schubert, R. Steinlechner *, R. de Oro Calderon

Technische Universität Wien, Institut für Chemische Technologien und Analytik, Getreidemarkt 9 – A-1060, Wien, Austria

ARTICLE INFO

Keywords:
WC-based cemented carbides
CoRu binder
Carbon processing window
W-solubility vs. C-activity
fcc-Co lattice parameter
WC grain growth
Eutectic melt formation

ABSTRACT

Our work confirms that the addition of Ru to Co-based cemented carbides significantly broadens the carbon processing window. Using a WC-10.9 wt% (Co-12.8Ru) alloy, the width of the two-phase window is extended from about 0.16 wt% C (Ru-free) to about 0.21 wt% C on addition of Ru.

According to semi-quantitative EDS analysis, the amount of W dissolved in the Co binder is significantly higher in Ru-containing materials at all carbon contents. This higher degree of solubility is also reflected in the lattice parameter. When decreasing the carbon content (from precipitation of graphite to the formation of eta carbides), the lattice parameter increases steadily from 3.585 Å to 3.609 Å respectively. In contrast, Ru-free materials present 3.548 Å in equilibrium with graphite, and 3.576 Å in equilibrium with eta carbides.

The relative magnetic saturation value of the alloys with Ru was significantly lower when compared to Ru-free alloys (from 80.2% at graphite precipitations to 41.4% with dendritic eta phase), which is also in agreement with the higher W solubility observed in these alloys.

DTA measurements of WC-4.4 wt% Ru-30 wt% Co samples (same Ru to Co ratio in the nominal composition) demonstrated a similar melting and solidification regime as compared to Ru-free WC-30 wt% Co materials.

1. Introduction and aim of the work

The following manuscript is focused on investigating the addition of moderate amounts of ruthenium (1.4 wt%) to a WC-9.5 wt% Co cemented carbide. The aim of this work is to demonstrate cobalt alloy formation in Ru containing alloys depending on carbon activity (carbon content), and to elucidate limits in accessible composition without forming unwanted additional phases. Furthermore, we discuss peculiarities of this system to improve our understanding of cemented carbides with Ru additions, used for milling and turning of difficult-to-machine materials.

2. Literature review on ruthenium in cemented carbides

2.1. The early story of ruthenium in cemented carbides until their commercialization in the late 1970s

The early history of ruthenium in cemented carbides starts in the late 1960s at Inco's European Research and Development Centre in Birmingham, UK [1]. At first considered as an alternative binder to cobalt (due to its high melting point) for the use in machining applications under especially arduous conditions [1–3], later research and development focused on the "old established PM route", adding fine Ru powder to the cemented carbide charge. Up to 50% of the cobalt was replaced by ruthenium [1].

Early on it was understood that ruthenium was forming solid solutions with cobalt, stabilizing its hexagonal crystal lattice [4]. It was considered that a hexagonal matrix in cemented carbides would impart lower friction characteristics (established for other hexagonal metals) resulting in less wear of the tools, providing a higher cutting speed and a longer tool life [1,5]. The next stage was to involve industry in exploiting the invention [5], and the first licensee, Higher Speed Metals Ltd., of Sheffield "started the production of many thousands of ruthenium alloyed cutting inserts during the 1970s" [6,7]. Further evaluations by other interested hardmetal manufacturers (including a second licensee, Stellram SA of Nyon, Switzerland) and further market evaluations led to the commercial introduction of the materials during June 1978/July 1979 [1,6,7].

At this stage of development, material properties reported in Journals were based on in-house testing and case studies in the related

* Corresponding author.
E-mail address: robert.steinlechner@tuwien.ac.at (R. Steinlechner).

https://doi.org/10.1016/j.ijrmhm.2023.106346
Received 21 April 2023; Received in revised form 5 July 2023; Accepted 21 July 2023
Available online 23 July 2023

industry, demonstrating the superior performance of Ru-containing grades - "*solving some of the roughest and most difficult machining problems in the engineering industry*". Most notable results were obtained in thread-machining and milling operations. The preliminary indications were that the optimum ruthenium content in cobalt should be 20 wt% (later reduced towards 15 wt% Ru), and the most notable increases in cutting performance were obtained with complex tungsten-titanium-tantalum grades; e.g., 6.8 wt% Co, 1.2 wt% Ru, 6 wt% TaC/NbC, 4.4 wt% TiC [1,6,7,9]. Ruthenium was also said to fill some of the high-performance gaps to which coatings cannot be applied [7]. It was hypothesized that the addition of Ru increases the toughness of the metallic binder and forms stronger bonds between the carbide particles and the matrix, inhibiting the propagation of cracks [8].

Despite the very high cost, ruthenium based cemented carbides have since then found their niche in the market, as the higher-priced tools aim to save in production costs [8].

2.2. Further research since 1980

Only a limited number of (open) scientific publications are available on ruthenium additions since their commercialization. This might be due to the niche role within the large market of cemented carbides as well as the high price of the metal additive (currently at about 14 € per g). Nevertheless, most large cemented carbide manufacturers provide such grades in their portfolio.

The first high temperature investigation on a Ru-containing cemented carbide is reported by Schmid et al. [10], based on the work of Bonjour [9], who had demonstrated that cemented carbide tools with approximately the same weight percentages of cobalt but with a small amount of ruthenium achieve much longer lifetimes. Specimens of WC-11 wt% Co-1.65 wt% Ru were tested under three-point bending conditions between 20 °C and 1000 °C. The authors reported a higher bending fracture stress of the Ru-containing material (3478 ± 170 MPa vs. 2450 ± 170 MPa for WC-11 wt% Co) at room temperature, and material creep is inhibited by the ruthenium additive. Both results were attributed to a reinforcement of the WC/WC and most likely also the WC-Co interfaces.

Lisovskii [11] reported the properties of a WC-15.5 vol% CoRu cemented carbide formed by metallic melt impregnation (MMI). The resulting compositing of the binder phase was 20.8 wt% Ru, 10.2 wt% W and 69.0 wt% Co. The alloying with Ru increased the bend, compressive, and yield strength of the cemented carbide. Ruthenium forms a solid solution with the binder phase [Co (Ru,W,C)], with a higher microhardness and elastic modulus than the solid solution [Co(W,C)]. Ru additions reduce the stacking fault energy of the cobalt phase and promote the transformation of the cubic structure of cobalt to the hexagonal. This results in precipitation hardening of the binder phase.

T.L. Shing et al. [12] reported on the effect of ruthenium additions on the hardness, toughness and grain size of WC-Co. The work compared WC-10 wt% Co cemented carbide with WC-Co-Ru alloys with additions of 0.4 wt% to 3 wt% Ru (i.e., 3.8 wt% to 23.1 wt% Ru in Co). The hardness of the WC-Co-Ru alloys increased with increasing Ru content while the toughness decreased. Substantial effects were found only when the Ru content was higher than about 15 wt%. The results indicated that the optimum Ru content in the binder of WC-Co-Ru alloys is approximately 15 and not 20 wt%, as estimated earlier by Tracey and Mynard [1]. The WC grain growth was slightly reduced by Ru, which supported the earlier observation reported by C. Bonjour [9].

In a subsequent manuscript, S. Luyckx [13] reported the hot hardness of WC-Co-Ru alloys, prepared and described in [12]. In conclusion, Ru additions increased the hot hardness of WC-Co alloys only within the temperature range where plastic deformation is controlled by the Co binder, since Ru is in solution in the binder and does not affect the composition and properties of the WC phase.

A further contribution of the South African research group described the results of a diffusion experiment in which Ru diffused into a WC-Co layer [14]. They observed that in this area the formation of eta phase in substoichiometric WC-Co was inhibited. The minimum amount of Ru required for the total inhibition of eta-phase was found to be ≥30 wt% Ru.

Two manuscripts by C. Bonjour [15,16] report increases in flexural strength in K-type and P30- type cemented carbides for a concentration of 15 wt% Ru in cobalt, whereas hardness only slightly varied. Ruthenium appeared to be an excellent grain growth inhibitor, which was explained by the Ru—Co phase diagram. Ruthenium-containing materials with about 13 wt% Ru in the nominal alloy composition (grades X11, X22, X33) exhibited a better impact resistance and a higher wear-resistance during both, turning and milling. Also, a more complex WC-10 wt% CoFeNi- 2 wt% Ru grade was investigated in their study [16].

In [17] P.K. Mehrotra and P. B. Trivedi present a contribution on the effect of metallic and non-metallic alloying additions to the cobalt binder in terms of phase composition, microstructure and selected physical and mechanical properties. The effect of binder composition on magnetic saturation is correlated with phase type and chemistry. Ru additions to WC-(9.5–11.5 wt%) Co alloys slightly increase hardness but decrease the transverse rupture strength as well as thermal conduction. In a further paper [18] the authors focus on ruthenium addition to cemented carbides. Ru additions expand the allowable carbon range of WC-Co without formation of undesirable eta-phase or graphite. The thermal conductivity is lower than that of WC-Co, and is further reduced in low carbon materials. Ru containing alloys depicted increased hot hardness compared to unalloyed WC-Co materials, and the effect remained intact up to a temperature of 800 °C. Ru additions also improved the performance of cemented carbide in both milling and turning applications.

Further information can be found in two recent US patents [19]. Referred cemented carbide articles exhibit enhanced resistance to wear and thermal fatigue, and can tolerate variations in carbon content without formation of undesirable phases, including eta phase and/or free graphite. In Table V of the patent the authors state an example composition, WC-9.5 wt% Co-1.5 wt% Ru. The patent shows, that in this material the carbon content could be varied over a large range, without the presence of eta phase or graphite. The carbon window of this material was assessed using measurements of the relative magnetic saturation and plotted vs. the carbon content and can be assessed from the drawing attached to the patent to be about 0.21 wt% C. Based on these patents, cemented carbides containing binder phases alloyed with Ru are fabricated on a large scale under the trade name X-GradeTM by Kennametal Inc.

Two different ruthenium-containing alloys (WC-6.5 wt% Co-11 wt% (W,Ti,Ta)C-0.5 wt% Ru; WC-6.5 wt% Co-11 wt% (W,Ti,Ta)C-1 wt% Ru) were prepared by X. Yang et al. [20] and compared to a Ru-free WC-6.5 wt% Co-11 wt% (W,Ti,Ta)C cemented carbide. The authors report a slightly increased hardness and transverse rupture strength of the Ru-containing materials and a more uniform microstructure with regard to local WC grain growth. Cutting tests demonstrated less flank wear of the ruthenium-containing materials.

L. Chipise et al. [21] investigated the sliding wear characteristics of WC-VC-Co alloys with various Ru additions and found optimal wear resistance for an 80 wt% WC-10 wt% VC-10 wt% Co-0.4 wt% Ru alloy.

Zhang et al. [22] added Ru (0.5 wt% to 2 wt%) to a WC-8 wt% Co cemented carbide and measured an increase in hardness and transvers rupture strength at 1.5 wt% Ru addition. Meanwhile, cemented carbides with 0.5 wt% Ru exhibited the highest toughness. Cemented carbide tools with Ru additions showed excellent cutting performance in dry cutting Ti6Al4V, and already a small amount of Ru addition was favourable for prolonging the lifetime of the tools; in particular, 0.5 wt% Ru. Both fcc Co and hcp Co were detected by X-ray diffraction, and the hcp fraction increased from 14.4% hcp without Ru to 39.6% with 2 wt% Ru addition, demonstrating the promotion of the hcp Co phase with increasing amounts of Ru. The lattice constant of the fcc phase increased from 3.563 Å (no addition) to 3.58 Å (0.5 wt% Ru), 3.582 Å (1 wt% Ru), 3.591 Å (1.5 wt% Ru) to 3.595 Å (2 wt% Ru). The existence of residual

stresses during cooling is attributed to induce the phase transition to hcp Co.

Recently, a study reported on the influence of carbon content on the binder microstructure in WC-15 wt% Co-2 wt% Ru cemented carbides [23] The authors describe an increase in coercivity and a decrease in magnetic saturation with decreasing carbon content, as a result of a higher tungsten content dissolved in the binder phase. The transformation from Co (fcc) to Co (hcp), observed by EBSD, was favoured with decreasing carbon, in samples subjected to slow cooling after sintering (2–3 °C/min). However, in materials with high cooling rate (15–20 °C/min) the carbon content seems to have a negligible influence on the formation of Co(hcp).

2.3. The binary system: cobalt/ruthenium [4]

Hexagonal cobalt and ruthenium form complete solid solution over the entire composition range. The maximum solubility of ruthenium in solid fcc cobalt is limited by the increase of the allotropic transformation temperature, and reaches a maximum value of about 16 at.% Ru at the formation of liquid. At higher Ru additions (25% to 30%) alloys are two-phase, with a cobalt-richer cubic phase and a ruthenium-rich hexagonal phase. Above 35 at.%, only hexagonal alloys are formed. The authors also describe a remarkable temperature hysteresis in the fcc Co → hcp Co transformation below 1000 °C.

The Curie temperature of the hcp phase is higher than that of the cubic phase, and the limit of the ferromagnetic area was determined as 34 at.% Ru.

2.4. Literature resumé

Besides its widespread use as a cutting material academic work on Ru-containing cemented carbides is limited over the last four decades. However, there are plenty of patents covering various use cases and compositions of this class of materials.

3. Experimental procedure

Four WC-9.5 wt% Co-1.4 wt% Ru cemented carbides were prepared with varying gross carbon content to provide information on phase formation in both low carbon and high carbon variants. This includes a sample with precipitations of eta phase, as well as a sample with graphite precipitations (see Table 1; alloys 1–4). The selected nominal composition of Ru refers to 12.8 wt% Ru of the binder (assuming all Ru is dissolved in cobalt). This composition corresponds to Stellram's earlier GX20TM grade and is close to the nominal composition of the material described in US Patent 9,725,794 B2 (2017) [19].

The individual carbon value of the samples ("weighted-in carbon") was adjusted by additions of C or W to cover the processing window of the system. Two Ru-free samples were prepared for comparison (WC-10.9 wt% Co; alloys 5 and 6), one with graphite, the other with precipitations of eta phase.

Standard grade powders of Co, Ru, W and C were used for alloy preparation (Fig. 1). A deagglomerated 3 μm FSSS WC powder was provided by Wolfram Bergbau und Hütten AG, Austria, exhibiting a rounded crystal shape. All powder grades are used in industrial production of hardmetals.

For the preparation of powder batches, the respective powders were mixed for 2 h in a Turbula mixer without wax. Pressing of the green parts was performed at 200 MPa. The parts were sintered in a semi-industrial GCA vacuum sintering furnace on yttria supports to prevent uncontrolled carbon pick up. The heating rate was 10 °C/min up to 1250 °C, and then 3 °C/min to the final hold: 1450 °C. The samples were placed in a graphite box together with WC-Co dummies to minimize carbon and cobalt losses during sintering. Soak time at the isothermal hold was 1 h. The cooling rate was about 15–20 °C/min down to 1200 °C. The total pressure was <0.01 mbar. Temperature measurement was performed by Pt-Pt/Rh thermocouples.

After sintering, two small pieces of alloy 3 (5x5x15 mm) were cut for quenching dilatometer experiments. A Quenching Dilatometer L78 RITA/Q (Linseis) was used. The first sample (alloy 7; Table 1) was heated to 1320 °C, kept at this temperature for 10 min, and then cooled down at ~100 K/s. The second sample (alloy 8; Table 1) was heated to the sintering temperature (1450 °C) and immediately cooled down at ~100 K/s. In both cases the samples were inductively heated under nitrogen at a rate of ~200 K/s.

Differential thermal analysis (DTA) measurements were carried out on WC-30 wt% Co-4.4 wt% Ru samples (12.8 wt% Ru in the nominal binder composition) to record the start of melting (during heating), as well as the start of solidification (during cooling). The compositions used considered WC-CoRu alloys containing graphite and eta phase formation, as well as a two-phase high carbon alloy. A carbon-saturated WC-30 wt% Co sample was used as an internal standard for comparison. DTA experiments were conducted using a Simultaneous Thermal Analyzer (STA) Netzsch STA 449C, using a heating and cooling rate of 20 K/min.

4. Characterization of the alloys

Sample cross sections were characterized using a Scanning Electron Microscope (SEM) FEI QUANTA 200 ESEM. Energy-Dispersive X-ray Spectrometry (EDS AMATEK Octane Pro) was used as a semi-quantitative method to identify differences in chemical composition. The binder composition was analysed in wider binder areas to minimize co-detection of the WC. An acceleration voltage of 20 kV was used in all measurements. Carbon was excluded from quantification when

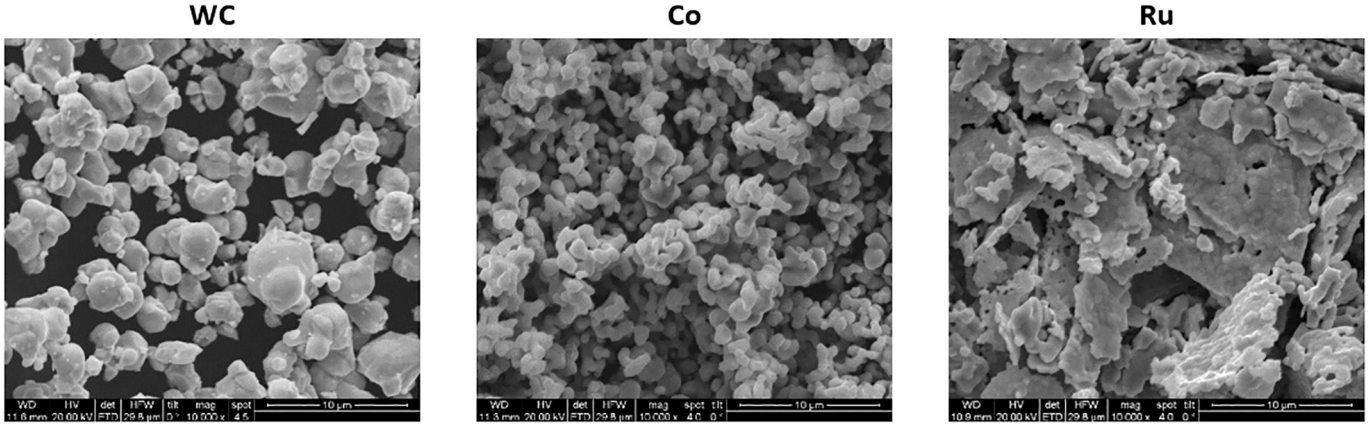

Fig. 1. SEM micrographs of the starting powders WC, Co and Ru.

measuring the composition of the binder phase. Point analyses were made in the center of large binder pools (5 μm to 10 μm in diameter) located in the core part of the samples, as possible surface decarburization/carburization might slightly alter the carbon content and therefore the solubility of the elements in the binder region located in the outer rim part of the samples. At least 5 different binder pools were measured on each sample in order to determine the average value with a scatter below 1 wt%. However, giving a confidence interval for this data is not possible as the values can be affected by the particular composition of the phase, the co-detection of other phases, the instrument used, the software and method used for quantification, etc. In any case, the values provided should only be taken as semi-quantitative.

X-Ray diffraction (XRD) was used to identify the phases in stress-free polished alloys, as well as for lattice parameter measurements of the fcc cobalt binder using a PANanalytical X'Pert PRO diffractometer (CuKα1 radiation). For the lattice parameter measurements, the WC peaks were used as an internal standard. To ensure adequate instrument resolution, LaB6 (NIST SRM 660b) was measured in the same setup as the samples. Alloys 1–6 were also etched electrochemically in a solution of 125 g Na_2CO_3 + 62.5 g Na-K-tartrate +62.5 g NaOH in 1000 ml H_2O at approximately +2 V potential and a current density of 50–80 mA/cm^2 for about 12 h to remove the WC prior to XRD measurement. The resulting binder networks (although slightly oxidised during etching) were also used for a comparative EDS analysis of the alloy binders 1–6. Etching is not uniform along the surface, the areas examined have an estimated etch depth of ~200 μm.

Magnetic saturation was measured using a Dr. Förster-Koerzimat magnetic analyzer and the coercivity was measured using a Koerzimat 1.097 HCJ device.

The hardness of the different alloys was determined on cross sections of the samples, following the norm ISO 3878. Indentations were made with a hardness tester M4U 025 by Emco (Austria) applying loads of 30 kgf and 50 kgf, respectively.

5. Thermodynamic calculations

A thermodynamic calculation based on the CALPHAD methodology was carried out for the comparative WC-10.9 wt% samples, and the result is used to discuss the constitution of the Ru-containing samples. The software ThermoCalc and the commercially available database TCFE9 were used. No calculations were made for the alloys containing Ru because Ruthenium does not exist in the TCFE9 database.

6. Results

A summary of the results of our investigation is presented in Tables 1 and 2.

Table 1 presents the nominal composition of our alloys 1–8, their "weighed-in" carbon content, as well as phase formation and solubility, determined experimentally by combining the results from our metallographic examinations, SEM-EDS and X-Ray diffraction patterns, according to the methodology described in previous publications [e.g., 24]. Alloys 1–4 have Ru-additions according to the nominal composition WC-10.9(Co-12.8Ru), alloys 5 and 6 are Ru-free comparative samples WC-10.9(Co), containing either graphite or eta phase besides WC and binder (Fig. 2). Alloys 7 and 8 are modifications of alloy 3. A small part of alloy 3 was cut and reheated to 1320 °C (alloy 7) and 1450 °C (alloy 8), and then quenched in a quenching dilatometer.

Table 2 presents the results of magnetic measurements (magnetic saturation, coercivity) on alloys 1–8, the hardness of the composites (HV30 and HV50), the mean intercept length of the WC as well as the lattice parameter of the fcc binder phase.

Fig. 3 demonstrates the results of our metallographic study in the form of SEM micrographs (alloys 1–6), also showing hardness (HV30) and WC mean intercept length values of the individual samples.

The results of our DTA measurements are presented in Table 3. Sample 1 represents a comparative material (internal standard), a graphite-saturated WC-30Co cemented carbide; sample 2, 3 and 4 are WC-30(Co-12.8Ru) materials, with varying gross carbon content covering the whole carbon window from graphite to eta phase formation. An example of a DTA run (sample 3 – two phase) is depicted in Fig. 4, indicating the onset of melt formation during heating, and the start of solidification during cooling.

A vertical section of the C-Co-W phase diagram, calculated at 10.9 wt % Co is shown in Fig. 5. On the basis of this phase diagram it is clear that in a WC-Co material, an alloy with 5.26 wt% C (nominal) would be expected to present massive eta carbides. However, this carbon content in a Ru-containing alloy (see alloy 4 in Fig. 2) resulted in the presence of only small amounts of dendritic eta carbides.

Table 1
Nominal compositions of Alloys 1–8 of this study, as well as results on phase analysis and binder compositions.

Alloy		Nominal C in wt%	Phases	W in binder	Ru in binder
1	WC-10.9(Co-12.8Ru)	5.90	WC, fcc, hcp, graphite	6.0 wt% / 2.1 at.%	10.1 wt% / 6.4 at.%
2		5.46	WC, fcc, hcp	15.7 wt% / 5.9 at.%	9.2 wt% / 6.3 at.%
3		5.36	WC, fcc, hcp	18.7 wt% / 7.1 at.%	7.6 wt% / 5.3 at.%
4		5.26	WC, fcc, hcp, eta	26.0 wt% / 10.5 at.%	8.3 wt% / 6.1 at.%
5	WC-10.9(Co)	5.90	WC, fcc, hcp, graphite	3.6 wt% / 1.2 at.%	–
6		5.31	WC, fcc, hcp*, eta	18.1 wt% / 6.6 at.%	–
7	Alloy 3 + Q-1320 °C	5.36	WC, fcc, hcp*	20.8 wt% / 8.1 at.%	8.0 wt% / 5.7 at.%
8	Alloy 3 + Q-1450 °C		WC, fcc	24.3 wt% / 9.7 at.%	7.7 wt% / 5.6 at.%

Q indicates quenching from the respective temperature; *phase fraction close to detection threshold.

Table 2
Properties of the binder and composite material.

Alloy	MS in μTm^3/kg	coercive field in kA/m	HV 30	HV 50	WC intercept length in μm	fcc-lattice parameter in Å
1	15.3 (80.2%)	5.309	1166	1108	2.8	3.585
2	12.1(63.3%)	5.372	1185	1195	2.8	3.597
3	9.0 (47.1%)	5.278	1190	1224	2.2	3.604
4	7.9 (41.4%)	8.252	1335	1280	2.1	3.609
5	20.6 (94%)	5.078	1063	1044	2.9	3.548
6	10.9 (49.7%)	6.961	1255	1264	2.2	3.576
7	–	–	–	–	–	3.62
8	–	–	–	–	–	3.622

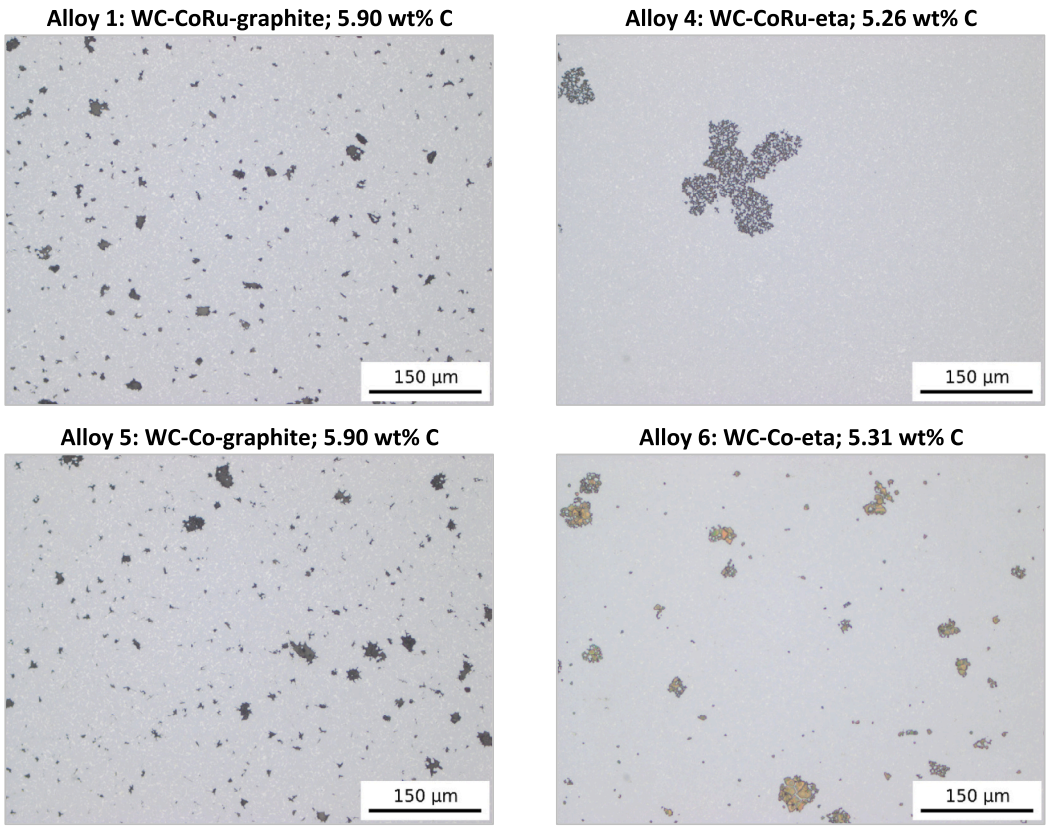

Fig. 2. LOM micrographs of alloy 1 and 5 (presence of graphite) und alloy 4 and 6 (presence of eta-carbides) after etching with Murakami for 3 s. The given carbon content presents the nominal C in the alloys.

7. Discussion

7.1. WC grain growth and grain shape

Previous investigations on adding Ru to WC-Co cemented carbides have described a WC grain growth inhibition effect during sintering, which was attributed to the Ru additive [9,12,15,16,21]. However, Fig. 3 suggests a different interpretation. From the series it is obvious that with decreasing the carbon content of the Ru-containing materials (at the same nominal composition; alloy 1 → 2 → 3 → 4), a decrease in mean WC grain size occurred. The lower the carbon content (i.e., the higher the amount of W in solution – see Table 1) the finer was the microstructure (i.e., the stronger the growth inhibition), with increasingly round WC grain shape. The strongest growth inhibition was obtained in alloy 4, which contained minor amounts of dendritic eta phase and depicted a clearly rounded WC grain shape (Fig. 3).

Alloys 5 and 6 (both Ru-free) also demonstrate a clear WC grain refinement with decreasing carbon (Table 1, Fig. 3), however the effect is less pronounced. Coercivity, mean WC grain size and HV30 values support this finding (Table 2). The strong influence of carbon on the growth of WC during liquid phase sintering in cemented carbides is well known [25], and was observed even in strongly growth-inhibited systems (e.g., in case of VC additions) [26].

These results indicate that it is not the Ru addition directly acting as a growth inhibitor. Rather, the measurements indicate that due to Ru addition the chemical composition of the binder phase changes. Ru addition - as indicated in Table 1 – increases the amount of W dissolved in the binder. The addition of Ru to cobalt obviously alters the composition of the growth environment during sintering. The lower the gross carbon (carbon activity), the stronger the growth inhibition.

7.2. Influence of the gross carbon content on cobalt alloy formation and composition

Table 1 summarizes the results of our phase analysis as well as the experimentally obtained W and Ru ("frozen-in") solubilities in the binder phase. Note that these measurements are based on a standard-free method (EDS), and thus cannot be regarded as quantitative. In addition, a certain degree of co-detection of the WC cannot be ruled out although care was taken by measuring in selected binder areas (coarse binder pools as described in [24]). Approximately 1 wt% of Ru was found in the eta carbides in the cross section of the sample. We expect this to be due to secondary X-ray fluorescence from the subjacent/intergrown binder. Analysis of the sintering skin of the sample, where large eta phases had grown into the free space, did not confirm Ru in the eta phase.

The results depicted in Fig. 6 show a striking increase in tungsten solubility in the Ru-containing alloy binder, from 6 wt% W in solid solution (alloy 1) to 26 wt% W in the eta phase containing material (alloy 4). These concentrations are much higher as commonly obtained in Ru-free grades, which is also supported by the results obtained from the Ru-free alloys 5 and 6 (3.6 wt% → 18 wt%; Table 1).

Alloys 7 and 8 (quenched from the solid resp. liquid phase) have a higher solubility of W than the comparable alloy 3. Solubility increases from 18.7 wt% W (cooling rate: 15–20 °C/min) to 20.8 wt% W (quenched from 1320 °C) and finally to 24.3 wt% W (quenched from liquid binder).

This strong increase in W solubility in cobalt is also supported by the strong decrease in magnetic saturation (Table 2), as already described by Trivedi and Mehrotra [17–19] as well as Olovsjö and Qvick [23], and by the strongly increasing lattice parameter of fcc cobalt (see Fig. 6). The solubility values obtained by EDS analysis of the binder refer to the binder overall composition, independently of whether fcc-Co and/or hcp-Co were present.

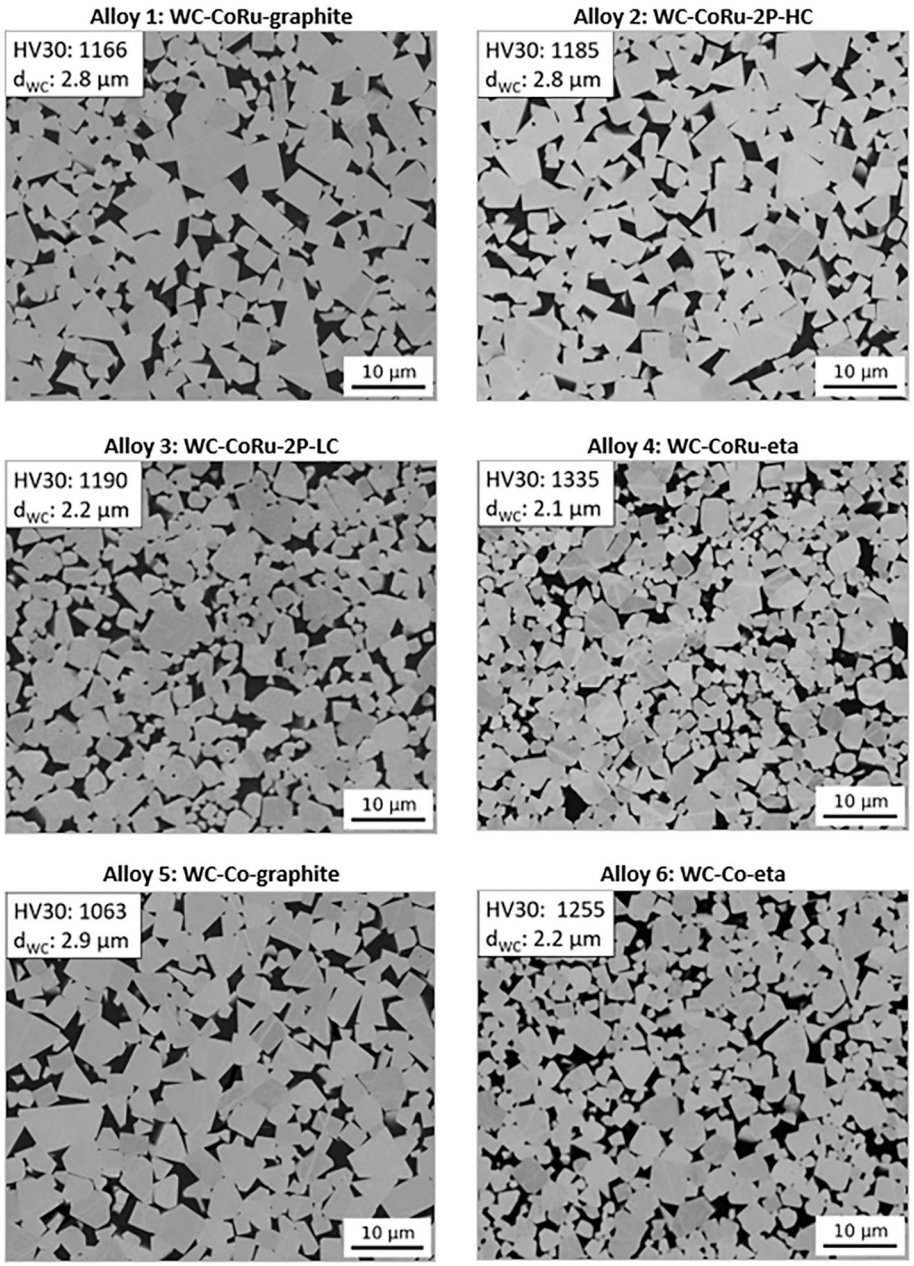

Fig. 3. SEM microstructures of alloys 1–6 (5000×); mean WC intercept length d_{WC} (µm) and hardness (HV30).

Table 3
Critical temperatures in °C for defining the melting and solidification regimes in DTA experiments. For more details on the calculation of these temperatures, see Fig. 4.

	Heating		Cooling	
	Onset	End	Onset	End
Sample 1 WC-30Co-graphite	1301	1325	1304	1286
Sample 2 WC-30(Co-12.8Ru)-graphite	1307	1335	1314	1293
Sample 3 WC-30(Co-12.8Ru)-2 phase	1329	1371	1351	1317
Sample 4 WC-20(Co-12.8Ru)-eta	1372	1425	1373	1329

7.3. EDS analysis of the binder networks obtained by electrochemical etching

The increase in W solubility in cobalt can also be observed in alloys 1–6 after electrochemical etching. As the WC is removed by the etching procedure, a binder network remains. The resulting porous network (Fig. 7) can be analysed by EDS, although the conditions for measurement (porous body, slightly oxidised metal binder during anodic dissolution) prevent quantification. However, EDS analysis of the networks clearly support the tendency in solubilities as obtained in the dense alloys (Fig. 8).

7.4. Influence of the gross carbon content on the fcc binder phase lattice parameter

XRD analysis of our alloys 1–6 demonstrates mainly fcc Co in both Ru-containing and Ru-free samples (Fig. 9). However, a certain amount

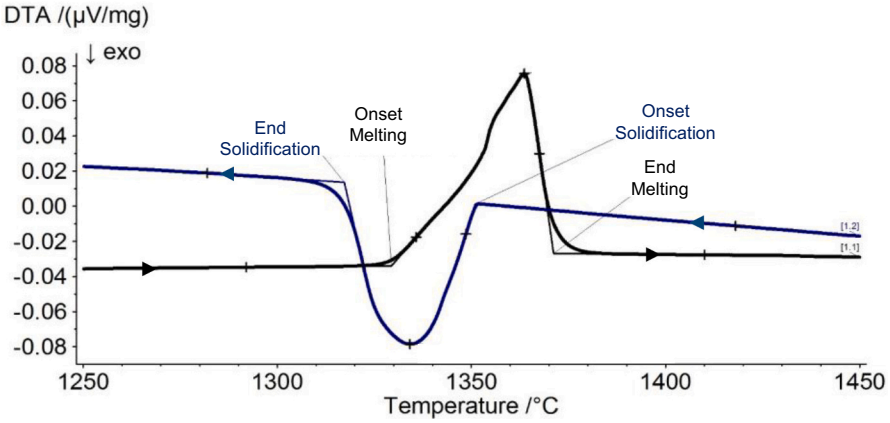

Fig. 4. DTA curves obtained for sample 3 (see Table 3). The image shows how the relevant temperatures were defined and calculated from the DTA measurement.

of hcp cobalt was always detected. In case of alloy 8, which was quenched from 1450 °C, the binder was fully fcc (Fig. 10), and the lattice parameter measured in this alloy (Table 1) was the highest of all of our alloys.

After electrochemical removal of the dominating WC phase in case of our alloys 1–6 the diffraction lines of the fcc and hcp Co appeared much clearer. The ratio between Co(fcc) and Co(hcp) showed to be similar (Fig. 11), with only one exception, alloy 6 which mainly presents fcc. Because of the broad diffraction lines a quantification of the fcc/hcp phase ratios was not carried out.

The lattice parameter of the fcc cobalt phase (obtained from non-etched alloys containing WC as an internal standard) increased from 3.585 Å (alloy 1) to 3.597 Å (alloy 2) further to 3.604 Å (alloy 3) to finally 3.609 Å (alloy 4). The value for the Ru-free alloys 5 and 6 varied between 3.548 Å (+graphite) to 3.576 Å (+eta). Alloys 7 and 8 (quenched) resulted in values of 3.62 Å, and 3.622 Å, respectively.

The lattice expansion is due to the formation of a solid solution of Ru,

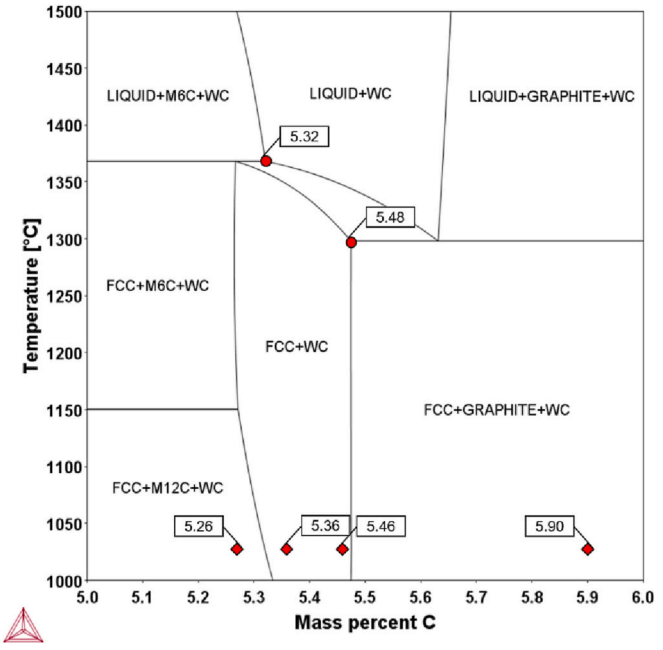

Fig. 5. Isopleth T vs C of the system WC-10.9 wt% Co. The red spheres indicate a carbon window of ΔC ≈ 0.16. The red squares below indicate our "weighed-in" carbon values of alloys 1–4 (Table 1). *Carbon shifts occur during processing, which in the current study (no powder milling) can be estimated to be ≤ 0.05 wt% carbon.* (For interpretation of the references to colour in this figure legend, the reader is referred to the web version of this article.)

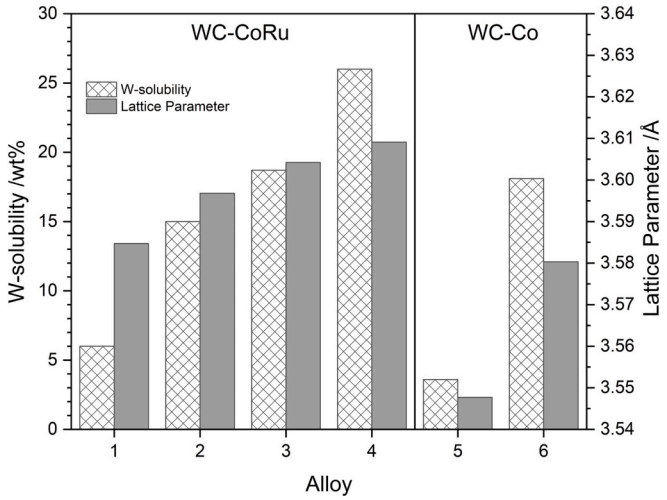

Fig. 6. W-solubility and lattice parameter values of alloys 1–6 in comparison; note the strong difference in lattice parameter between alloy 1 and alloy 5 (both with massive graphite precipitations).

W and C in fcc cobalt (i.e., the frozen-in composition [27]). Lattice parameter of CoRu-solid solutions were published by Köster and Horn [4]. A steady increase was observed with increasing Ru content from 3.544 Å (pure Co) to 3.58 Å for a (Co20 at.% Ru) solid solution. Taking these values and calculating values for a solid solution of 12.8 wt% Ru in cobalt (i.e., considering a solution of about 7.8 at.% Ru in cobalt) a lattice parameter of about 3.558 Å is obtained. This value is significantly lower than the value obtained in our alloy 1 (3.585 Å – precipitations of graphite). Thus, increases in lattice parameter are due to the enhanced additional solution of W (and likely also C) in the cobalt binder. This trend is also seen with the significant increase of the lattice parameter in alloys 7 and 8 (quenched) as compared to alloy 3 (furnace cooling).

The results indicate that the Ru addition increases the amount of W in solid solution over the whole carbon range studied, i.e., over the existing carbon window, and demonstrate an increase in W-content with decreasing C-activity, until eta phase is formed. The results also explain the diffusion experiments of Shing et al. [14], who reported Ru to act as an"eta-phase inhibitor" in WC-Co.

The significant increase in lattice parameter of alloy 1 compared to alloy 5 (both exhibiting substantial precipitations of free graphite; Fig. 6) seems to be a peculiarity of the Ru-system. The data might indicate that upon cooling of alloy 1 a tungsten-richer fcc cobalt phase is formed together with a Ru-richer hcp phase. In contrast, in alloy 5 the measured lattice parameter suggests martensitic transformation of the binder.

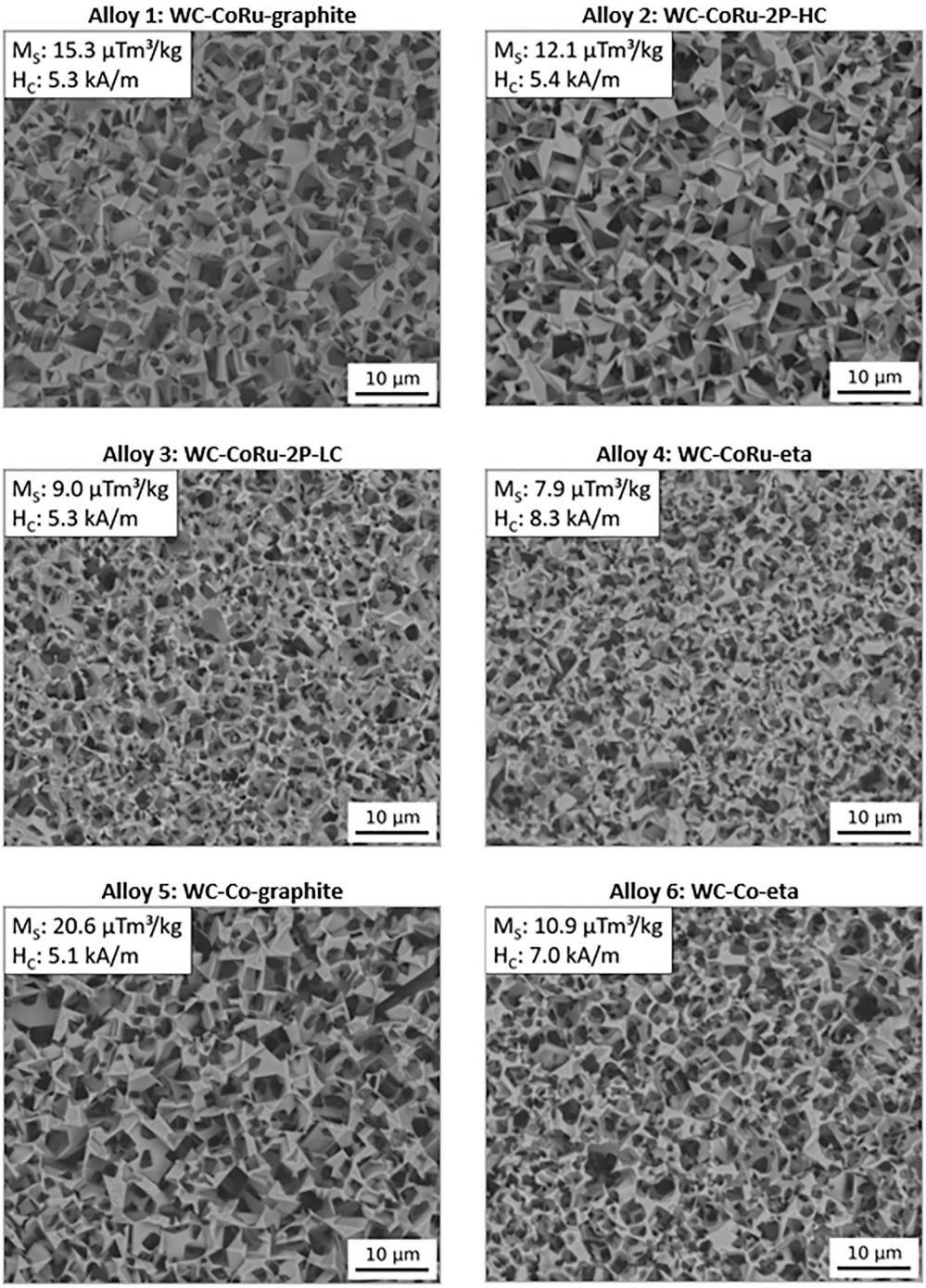

Fig. 7. SEM micrographs of alloys 1–6 after electrochemical etching of the WC with magnetic saturation values (M_S) and coercivity values (H_C) of the hardmetal specimen prior to etching.

7.5. The carbon window of WC-10.9 wt% (Co-12.8 Ru) cemented carbides

The width of the carbon window of a cemented carbide system is an important parameter, in particular for manufacturing. It is determined by phase equilibria prevailing in the respective systems, and indicates, whether or not a two-phase material (WC + alloy binder) is obtained after sintering, or, whether substoichiometric carbides or graphite are additionally formed.

This is demonstrated in Fig. 5 for the calculated WC-10.9 wt% Co system. The carbon window is indicated as the area between the two limiting red spheres and can be red out as $\Delta C \approx 0.16$, a value which matches practical experience quite well.

Measuring the width of the carbon window in a new system -as for example our WC-10.9(Co-12.8Ru) cemented carbide- represents a laborious study. A large number of alloys with varying carbon contents are needed, and the carbon content is measured precisely after the sintering process. This is mandatory, as during sintering on the laboratory scale carbon loss will occur, shifting the intended carbon concentration lower.

In our study, we have sintered four different Ru-containing alloys, a number not sufficient for assessing the isopleth in the system. However, in our sample set we observe that −0.20 wt% C difference between alloy 2 (stoichiometric carbon) and alloy 4 produced a material with only a

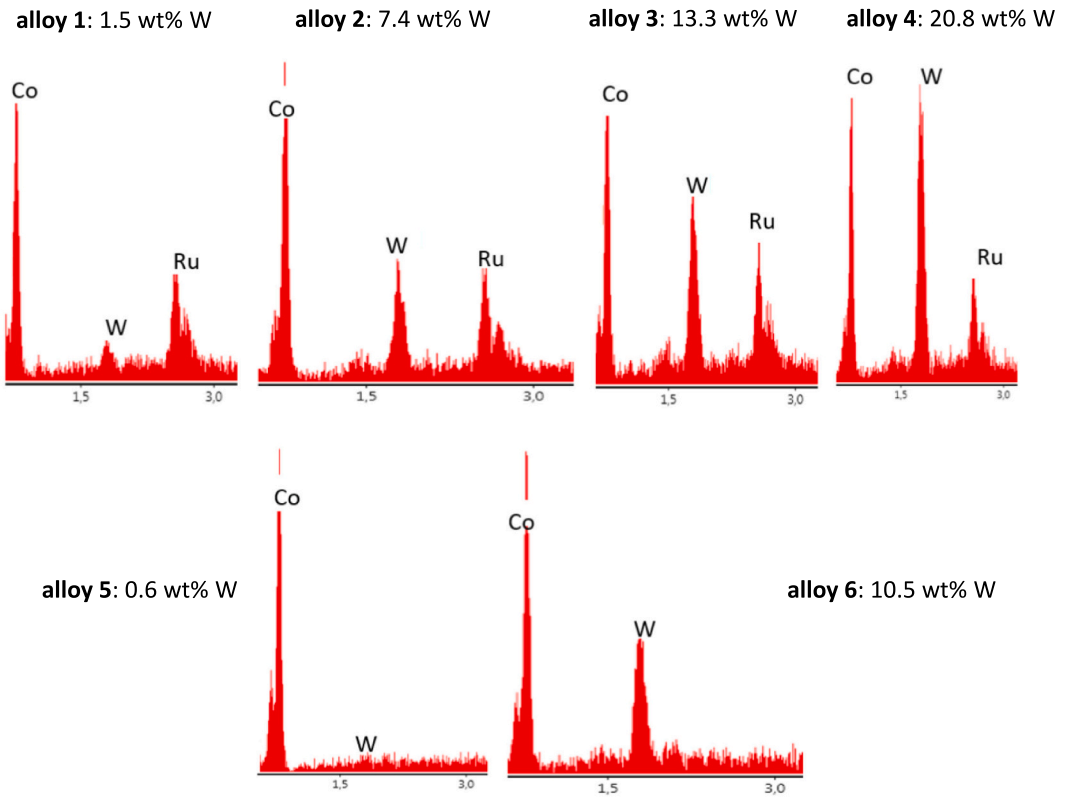

Fig. 8. Part of the EDS emission spectra of alloys 1–6; measured on the binder network obtained by alkaline etching (Fig. 7). Although not quantitative, the series reflect the significant differences in W solubility both in the Ru-containing and Ru-free alloys. During etching, the metal network passivates and forms a thin oxide layer which complicates the measurement. Oxygen is not considered in analysis.

minor amount of dendritic eta carbides present (see Fig. 2 and Fig. 9), although massive eta carbide formation was intended. In contrast, in alloy 6 (Ru-free), only −0.15 wt% C from the stoichiometric carbon (i.e., 5.46 wt% C) resulted in comparable amounts of eta carbide under the same preparation conditions (see Fig. 2 and Fig. 9). This result indicates that the Ru-containing carbon window is extended towards lower carbon values of the system.

A thorough literature research helped us in further evaluating the system. Trivedi and Mehrotra [18,19] have already shown that Ru additions broaden the carbon window of Ru-containing cemented carbides, and have demonstrated it for a WC-9.5Co-1.5Ru compositions. The window was established by coercivity measurements of samples with precisely measured carbon and was demonstrated to be about $\Delta C \approx 0.21$.

As the system described by the authors is very similar to our nominal alloy composition (i.e., WC-9.5Co-1.5Ru) we can compare their material with our materials, in using a calculated isopleth of their basic system (WC-11% Co), Fig. 12.

Comparing Fig. 5 (our system) and Fig. 12 (their system) one immediately sees that the isopleths are nearly identical and the calculated carbon window has not changed significantly (as it was expected because the only difference is a change in the amount of WC from 89.1 wt% C to 89 wt% WC). For both systems the window remains at about $\Delta C \approx 0.16$ for Ru-free alloys.

In addition, Fig. 12 includes information about the width of the carbon window of the Ru-containing materials, in the form of two violet chain-dotted lines. This information was taken from the work of Trivedi and Mehrotra [19]. One clearly discerns that the change in carbon window is significant, and the window of the Ru-containing materials (WC-9.5Co-1.5Ru; WC-9.5Co-1.4Ru) is primarily extended towards the low carbon side, with a slight increase towards the higher carbon side when compared to the plain WC-11 wt% Co and WC-10.9 wt% Co materials.

Based on the work of Trivedi and Mehrotra [19] and in agreement with our experimental findings we can therefore conclude that a carbon window of $\Delta C \approx 0.21$ is a reasonable estimate for our WC-10.9(Co-12.8Ru) cemented carbide. The confirmation of the broadening of the carbon window provided in this work stems not only from the microstructural examinations, but also from the solubility studies. The considerably higher W content measured in Ru-containing low carbon samples (alloy 4 with 26 wt%W) as compared to equivalent Ru-free materials (alloy 6 with 18 wt% W) indicates that Ru-containing binders will require larger sub-stoichiometric compositions in order to get saturated in W and thus enable the precipitation of eta-carbides.

7.6. *Structure of the binder phases without and with Ru additions*

7.6.1. *WC-Co*

In WC-Co based cemented carbides the cobalt binder phase is present as face-centred cubic (fcc) grains but also in the (low temperature) hexagonal close-packed form (hcp). One can expect fcc-Co to form during solidification of the melt as large grains (commonly in the range of several tenths to hundreds of μm), which on further cooling either retain a fcc-binder structure, or partly transform into finer, hcp crystal units (formed within the larger fcc grains) [23,28]. Mingard et al. [28] have shown by EBSD mapping that this transformation almost fully occurs with a $\{111\}_{fcc}//\{0001\}_{hcp}$ orientation relationship.

Several parameters influence this fcc/hcp martensitic transformation, such as composition, microstructural features (WC grain size, binder phase volume), stresses formed during cooling (cooling rate) or annealing. Both W and C are considered to stabilize the fcc phase, but recent work has shown that the stabilizing effect of W depends on its concentration [29]. In addition, Mingard et al. [28] have revealed that there is no trend with Co structure in cemented carbides and examples

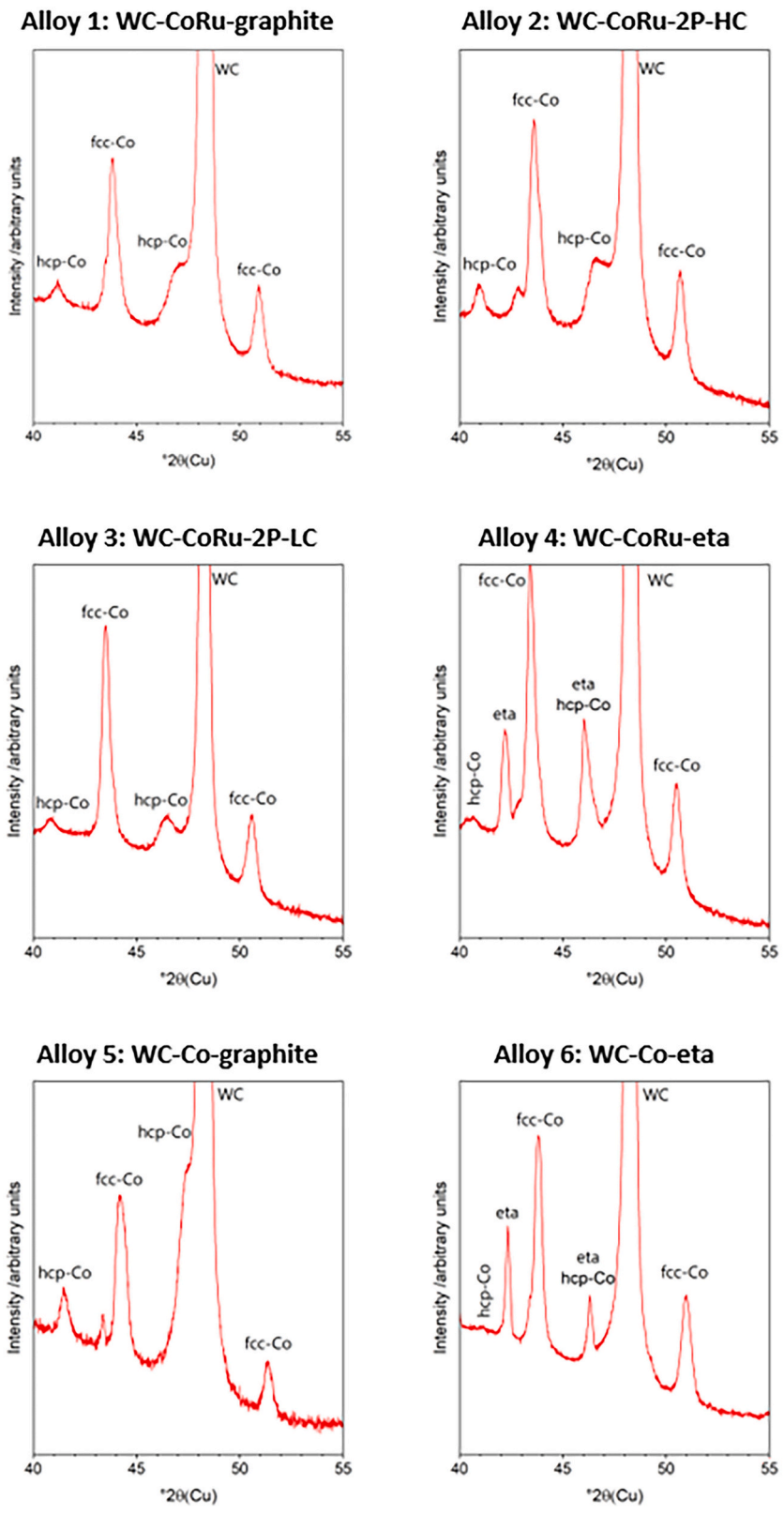

Fig. 9. XRD patterns of alloys 1–6 after stress-free polishing.

were given of similar tungsten concentrations in solid solution but structures to be either nearly fully fcc, or, mainly hcp. The authors also investigated the influence of sample preparation on fcc/hcp transformation (prior to EBSD measurement) and confirmed that the ratio of the structures did not alter in samples due to mechanical polishing, as one might expect from a strain-induced fcc/hcp martensitic transformation, as occurs during binder deformation [30].

Despite the importance of cemented carbides as tool materials there is still limited knowledge about how the fcc/hcp content (ratio) influences deformation and fracture characteristics (monotonic or cyclic loading) [28].

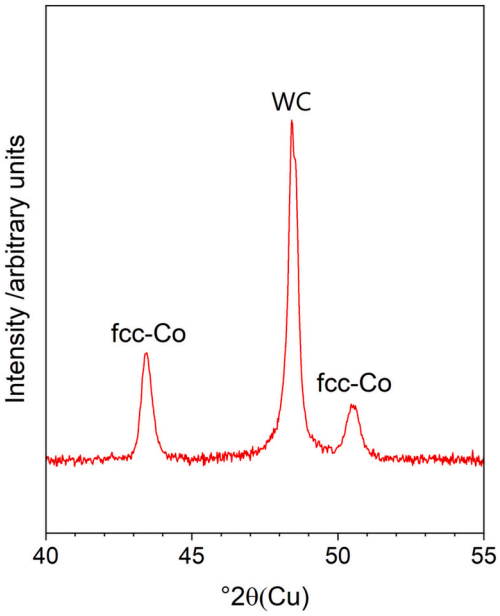

Fig. 10. XRD pattern of alloy 8 in a quenched state after stress-free polishing.

7.6.2. WC-Co(Ru)

Ruthenium metal exhibits a hexagonal close-packed (hcp) crystal structure and additions of Ru to cobalt were shown to stabilize the low-temperature hcp cobalt lattice [4]. In addition, a first principles study of the stacking fault energies for fcc Co-based binary alloys demonstrated that Ru additions promotes the hcp phase formation [29].

Whereas it is quite clear that hcp Co will form at higher Ru additions (> 45 wt% Ru) [4], a two phase fcc/hcp binder structure is expected at lower additions. According to the binary phase diagram Co—Ru [4] fcc Co is formed on solidification at compositions <25 wt% Ru but will transform partly into hcp cobalt on cooling in the solid state. Köster and Horn [4] have revealed that in this case an equilibrium between fcc and hcp phase will form until below 1000 °C martensitic transformation occurs. This indicates that above this temperature two solid binder phases will coexist with different concentrations (molar volumes); i.e., a more Co-rich fcc phase and a more Ru-rich hcp phase.

Lisovskii [11] observed a mixed fcc/hcp binder structure in a cemented carbide with a Ru content of 20.8 wt%. This binder had a significantly higher nano-hardness as the Ru-free WC-Co comparative alloy (7.1 GPa instead of 5.8 GPa). He explained this increase by precipitation hardening of the binder phase (in addition to solid-solution hardening). Zhang et al. [22] have recently demonstrated that the amount of hcp phase increased from 14% (ruthenium-free) to 40%

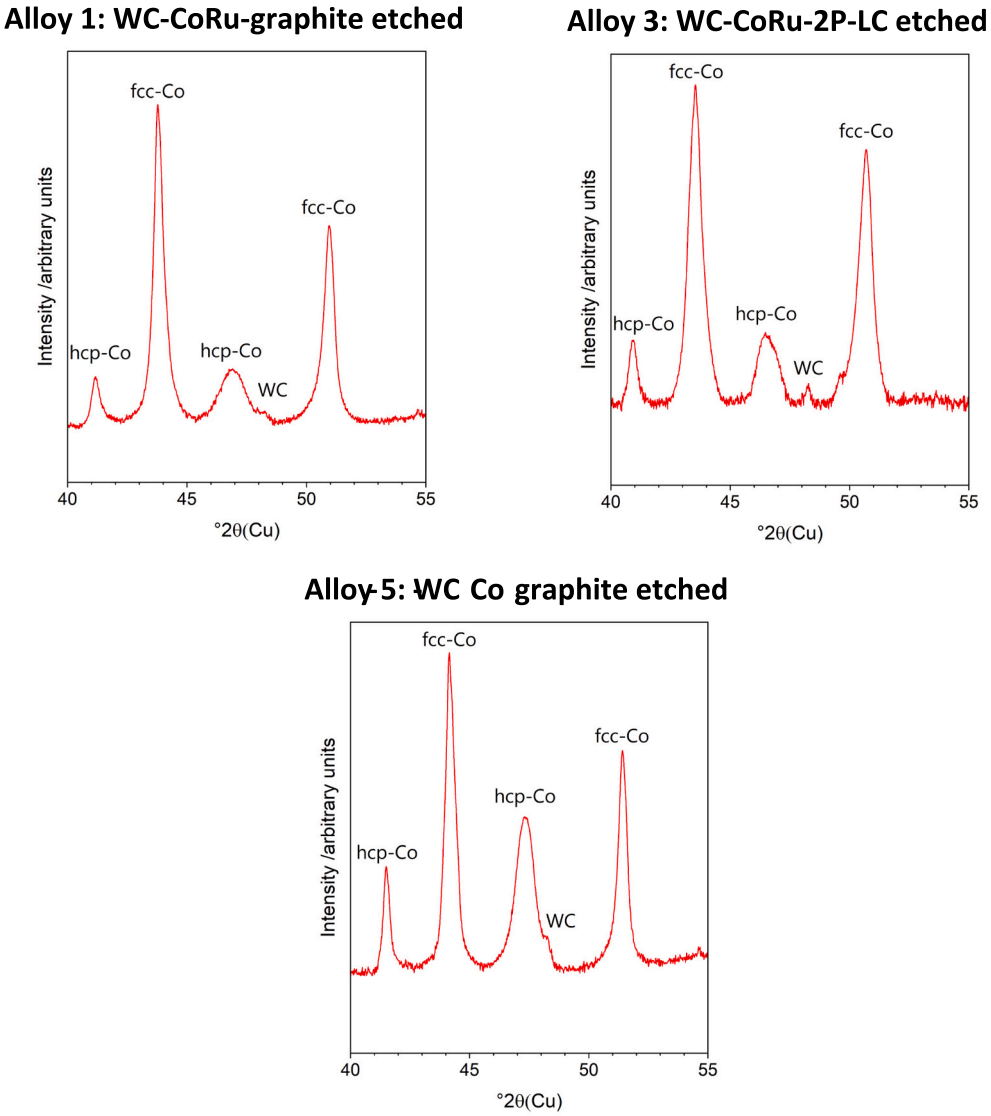

Fig. 11. XRD patterns of alloys 1, 3 and 5 after removal of WC via electrochemical leaching.

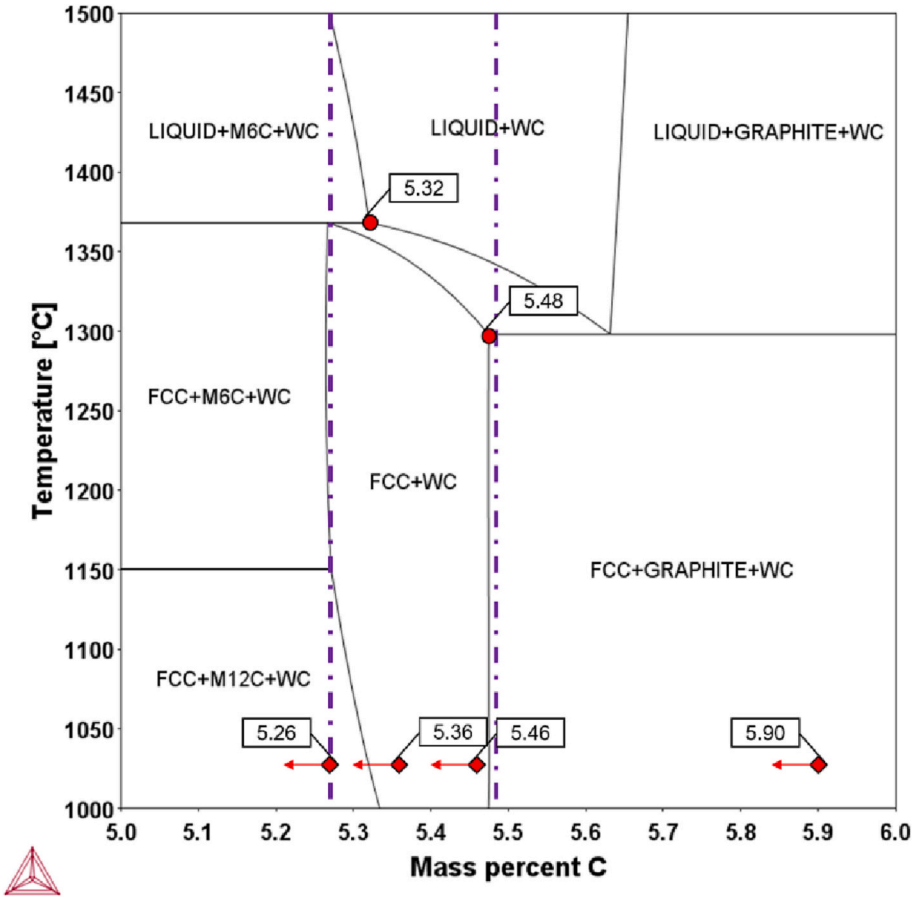

Fig. 12. Isopleth T vs wt% C of the system WC-11 wt % Co. The red spheres indicate a carbon window of $\Delta C \approx 0.16$ (see also Fig. 5). The chain-dotted violet lines demonstrate the results of the work of Trivedi and Mehrotra on a WC-9.5 wt% Co-1.5 wt% Ru cemented carbide [19]. Within these lines the authors observed WC and Co binder, only. A clearly extended carbon window can be derived from this presentation ($\Delta C \approx 0.21$). The red arrows below show the individual carbon values of our alloys 1–4 ("weighed in"), and their probable shift in carbon during sintering (burn-off). (For interpretation of the references to colour in this figure legend, the reader is referred to the web version of this article.)

(Co20 wt% Ru) in their WC-8 wt% CoRu alloys. The authors explained this difference by the fact that during cooling Ru promoted the phase transition from fcc to hcp.

Most of the work published on Ru additions to cemented carbides refer to Ru additions ≤15 wt% Ru, as machining tests had shown superior performances in this composition range. However, only three investigations [18,19,23] have considered variations in carbon in the investigated system; i.e., the formation of different alloy compositions, which not only influences solid solution strengthening but most probably also the fcc/hcp ratio (and probably precipitation hardening) during cooling.

Olovsjö and Qvick [23] reported that in their EBSD investigation on carbon variations in a WC-17 wt% (Co11.8 wt% Ru) cemented carbide the ratio of hcp/fcc significantly increased from 0.68 in a high carbon material to 4.5 in a low carbon material at slow cooling rate (3 °C/min). This ratio was, however, changed on fast cooling (15–20 °C) to 0.22 (HC) and 0.09 (LC) alloy. This demonstrates a clear impact of the thermal history on phase formation in Ru-containing cemented carbides (as one might expect from the binary phase diagram Co—Ru).

In our investigation using WC-10.9 (Co-12.8 wt% Ru) cemented carbides we observed roughly the same fcc/hcp phase ratio over the carbon range studied. This might be due to the high cooling rate in our investigation (15–20 °C/min). The majority binder phase structure was always fcc. The diffraction lines of hcp Co were strikingly broad, which reflects small crystallite sizes, residual stresses and/or compositional non-uniformities formed during cooling.

WC-Co(Ru) hardmetals might be interesting candidates for annealing experiments, as one might expect precipitation hardening on forcing the fcc/hcp transition at elevated temperatures.

7.7. Magnetic saturation

The values of magnetic saturation of our Ru-containing samples (Table 2) strongly decreased from 15.3 $\mu Tm^3/kg$ (+graphite) to 7.9 $\mu Tm^3/kg$ (+eta). In addition, the individual values were significantly lower as one would expect from comparison to Ru-free samples at the same C and Co content. Related to the magnetic saturation of pure cobalt for our composition this results in % values of 80.2% (+graphite), 63.3% (two phase; MC), 47.1% (two phase; LC) and 41.4% (+eta). Obviously, the low values are due to the very high solubility of W and Ru in solid solution.

Olovsjö and Qvick [23] reported similar results in their investigation on WC-17 wt% (Co-11.8Ru) cemented carbides. They also demonstrated that a higher cooling rate further reduced the values, and explained this with a higher amount of W in solid solution.

A strong decrease in magnetic saturation by additions of Ru is also mentioned in [19], in which the percentages of magnetic saturation (MS, %) were related to the individual (measured) carbon content of WC-9.5 (Co13.6Ru) cemented carbides. The values varied between roughly 82% at the occurrence of graphite, and about 47% at formation of eta carbides.

In practice, the values of magnetic saturation depend on several factors, such as microstructural and compositional parameter, cooling rate and also on the presence of hexagonal Co, i.e., the ratio of fcc/hcp binder structures. It is known, that Curie temperature of fcc and hcp Co (Ru) are not the same [4].

According to B. Cole [7] the low magnetic saturation of Ru-bearing materials was already known in the early time of alloy development, and was seen as a peculiarity of the materials.

7.8. Formation of liquid phase in Ru-containing cemented carbides

Eutectic melt formation in Ru-containing carbides is not discussed in the literature. Reference [12] indicates that a sintering temperature of 1410 °C was too low to provide dense samples containing 16.7 wt% Ru in Co. Based on this information 1450 °C was used in our sintering study.

To gain a better insight into the formation of liquid phase during sintering, DTA measurements were carried out on WC-30 wt% (Co-12.8Ru) materials with differing gross carbon (Table 3; samples [2–4]). As an internal standard, a Ru-free, carbon saturated WC-30 wt% Co sample was used (sample 1). This sample was used as standard since the temperature of the four-phase equilibrium (fcc + WC + graph. + L) in the C-Co-W system is well known (1298 °C [31]).

The results demonstrate that in Co-12.8Ru cemented carbides the melting and solidification behaviour is about the same as in Ru-free WC-Co cemented carbides, both at high and low carbon concentrations. There is a shift of a few degrees only (~6 °C), between our internal standard and the Ru-containing, carbon-saturated sample 2 in terms of melt formation on heating. Also, the start of melting on heating and the start of solidification on cooling of sample 4 (containing eta) are shifted only a few degrees above the temperature of the four-phase equilibrium (fcc + WC + M_6C + L); i.e., 1368 °C [31]. These temperatures are well below our selected sintering temperature of 1450 °C.

8. Conclusions

The experiments presented in this manuscript support the following conclusions:

- Microstructural examinations and W solubility measurements confirm that larger sub-stoichiometric compositions are necessary in Ru-containing binders to promote the precipitation of eta carbides. This, in turn, means that the addition of 1.4 wt% Ru to a WC-9.5 wt% Co cemented carbide significantly widens the carbon window of the materials. The results are in excellent agreement with those of Trivedi & Mehrotra [19] who reported an expansion from about ΔC ≈ 0.16 wt% in Ru-free alloys to about ΔC ≈ 0.21 wt% in Ru-containing alloys.
- The addition of Ru increases the binder solubility of tungsten in solid solution over the carbon range studied (from about 6 wt% W at presence of graphite to 26 wt% W at presence of eta phase).
- The increasing degree of W-alloying is reflected by a steady increase of the lattice parameter of fcc cobalt from 3.585 Å (presence of graphite) to 3.609 Å (presence of eta phase).
- The magnetic saturation of the Ru grades is significantly decreased from about 80% (+graphite) to 41% (+eta); related to pure cobalt. This again reflects the high amount of Ru and W in solid solution.
- The coercivity of the Ru-containing alloys increased with decreasing carbon, indicating a decrease of WC grain size of the cemented carbide. This is in accordance with a significantly finer WC microstructure, a smaller WC mean intercept length, and a higher hardness of the substoichiometric materials. The growth inhibition is mainly governed by the carbon content, and only indirectly by the Ru addition.
- The binder structure consisted of mainly Co(fcc), but Co(hcp) was present in all our samples. The diffraction lines of the hcp crystals were broad, indicating small crystallite sizes, stresses and/or compositional non-uniformities, formed on cooling.
- The solidus and liquidus temperatures of the Ru-containing materials are only slightly increased in comparison to Ru-free WC-Co cemented carbides.

Declaration of Competing Interest

The authors declare that they have no known competing financial interests or personal relationships that could have appeared to influence the work reported in this paper.

Data availability

Data will be made available on request.

Acknowledgements

Dr. Edward Sachet (Third Floor Materials, Raleigh, NC) is gratefully acknowledged for critical discussions and for his support during preparation of this paper. We also thank Dipl.-Ing. Werner Artner and Dr. Erich Halwax for their help in carrying out lattice parameter measurements. The authors acknowledge TU Wien Bibliothek for financial support through its Open Access Funding Programme.

References

[1] V.A. Tracey, B.A. Mynard, Development of Tungsten Carbide-Cobalt-Ruthenium cutting tools for machining steels, in: H.H. Hausner, H.W. Antes, G.D. Smith (Eds.), Modern Developments in Powder Metallurgy: Proceedings of the 1980 International powder metallurgy conference vol. 14, 1980, pp. 281–292. Washington, DC.
[2] R. Warren, M.B. Waldron, The microstructure and properties of sintered TiC-Ru alloys, in: 8th Plansee Seminar Vol. 2, 1974, pp. 1–14, 32.
[3] J.S. Jackson, R. Warren, M.B. Waldron, Cemented carbides with high melting-point precious metal binder phases, in: 8th Plansee Seminar vol. 2, 1974, pp. 1–15, 33.
[4] W. Köster, E. Horn, Zustandsbild und Gitterkonstanten der Legierungen des Kobalts mit Rhenium, Ruthenium, Osmium, Rhodium und Iridium, Int. J. Mater. Res. 43 (12) (1952) 444–449.
[5] B.A. Mynard, B. Jones, V.A. Tracey, W. Betteridge, Ruthenium or osmium on hard metal, United States Patent 3,785,783 (1974).
[6] K. Brookes, Ruthenium boosts carbide's capability, Metalwork. Prod. (1978) 13.
[7] B. Coles, (formerly at Marshalls Hard Metals), B. Roebuck (NPL); private communication, 2023.
[8] K. Brookes, Ruthenium exploits its precious talent, Metalwork. Prod. (1979) 77–80.
[9] C. Bonjour, Nouveaux Développments dans les outils de coupe en cárbure fritte, Wear 62 (1980) 83–122.
[10] H.G. Schmid, D. Mari, W. Benoit, V. Bonjour, The mechanical behaviour of cemented carbides at high temperatures, Mater. Sci. Eng. A 106 (1–2) (1988) 343–351.
[11] A.F. Lisovskii, Cemented carbides alloyed with ruthenium, osmium, and rhenium, Powder Metallurgy and Metal Ceramics 39 (9–10) (2000) 428–433.
[12] T.L. Shing, S. Luyckx, I.T. Northrop, I. Wolff, The effect of ruthenium additions on the hardness, toughness and grain size of WC-co, Intern. J. Refract. Metals & Hard Materials 19 (2001) 41–44.
[13] S. Luyckx, High temperature hardness of WC-co-Ru, J. Materials Science Letters 21 (2002) 1681–1682.
[14] T.L. Shing, R.H. Eric, S. Luyckx, Ruthenium as an eta-phase inhibitor in WC-Co, PM, in: Structure and Properties (2), 2002, pp. 92–99.
[15] C. Bonjour, Effects of ruthenium additions on the properties and machining behaviour of WC-Co hard metals, Euro PM, in: PM Tool Materials, vol. 3, 2004, p. 529.
[16] C. Bonjour, A. Actis-Data, Effects of ruthenium additions on the properties of WC-Co ultra micrograins, in: Euro PM, PM Tool Materials, vol. 3, 2004, pp. 543–549.
[17] P.K. Mehrotra, P.B. Trivedi, Effect of binder composition on cemented carbides, in: Powdermet 2015, 2015 International Conference on Powder Metallurgy & Particulate Materials, MPIF, San Diego, 2015.
[18] P. Mehrota, P. Trivedi, G. Roder, Recent advances in ruthenium containing hardmetals, in: World PM2016 – HM Processing II, 2016, pp. 1–6.
[19] P. B. Trivedi, P. K. Mehrotra, US Patent 9,725,794 B2 (2017); US Patent 10,415,119 B2 (2019).
[20] X. Yang, Q. Tang, X. Zhang, J. Shu, J. Liao, Effect of ruthenium on microstructure and properties of WC-(W, Ti, ta)C-co cemented carbide, Mater. Sci. Forum 8993 (2019) 851–856.
[21] L. Chipise, P.K. Jain, L.A. Cornish, Sliding wear characteristics of WC-VC-co alloys with various Ru additions, International Journal of Refractory Metals & Hard Materials 95 (2021), 105429.
[22] H. Zhang, J. Xiong, Z. Guo, T. Yang, J. Liu, T. Hua, Microstructure, mechanical properties, and cutting performances of WC-co cemented carbides with Ru additions, Ceramic International 47 (2021) 26050–26062.
[23] S. Olovsjö, J. Qvick, Influence of carbon content on the binder microstructure in WC-co-Ru cemented carbides, 20th international Plansee seminar, HM 116 (1–7) (2022).
[24] R. Steinlechner, R. de Oro Calderon, T. Koch, P. Linhardt, W.D. Schubert, A study on WC-Ni cemented carbides: constitution, alloy compositions and properties, including corrosion behaviour, Intern. J. Refract. Metals & Hard Mater. 193 (2022), 105750.
[25] J. Gurland, A study of the effect of carbon content on the structure and properties of sintered WC-co alloys, Transactions AIME, Journal of Metals (1954) 285–290.

[26] W.D. Schubert, Kornwachstum und Kornwachstumshemmung in Hartmetallen - eine ganzheitliche Betrachtung, 23. Hagener Symposium, Fachverband Pulvermetallurgie, ISBN 3–933842–79-4, 2004, pp. 117–139.
[27] M. Walbrühl, D. Linder, J. Ågren, A. Borgenstam, Diffusion modeling in cemented carbides: solubility assessment for co, Fe and Ni binder systems, International Journal of Refractory Metals & Hard Materials 68 (2017) 41–48.
[28] K.P. Mingard, B. Roebuck, J. Marshall, G. Sweetman, Some aspects of the structure of cobalt and nickel binder phases in hardmetals, Acta Mater. 59 (2011) 2277–2290.
[29] L.-Y. Tian, R. Lizárraga, H. Larsson, E. Holmström, L. Vitos, A first principles study of the stacking fault energies for co-based binary alloys, Acta Mater. 136 (2017) 215–223.
[30] C.H. Vasel, A.D. Krawitz, E.F. Drake, E.A. Kenik, Binder deformation in WC-(Co,Ni) cemented carbide composites, Metallurgical Transaction A 16A (1985) 23092317.
[31] O. Kruse, B. Jansson, K. Frisk, A revised thermodynamic description of the co-W-C system, Journal of Phase Equilibria 26 (2005) 152–160.